26th EPS Conf. on Contr. Fusion and Plasma Physics, Maastricht, 14 - 18 June 1999 ECA Vol.23J (1999) 1473 - 1476

H-Mode Phenomenology in W7-AS Configurations Bounded by Magnetic Islands

P. Grigull, M. Hirsch, K. McCormick, J. Baldzuhn, R. Brakel, S. Fiedler, Ch. Fuchs, L. Giannone, H.-J. Hartfuss, D. Hildebrandt, J. Kisslinger, R. König, G. Kuehner, H. Maaßberg, F. Wagner, W7-AS Team

Max-Planck-Institut für Plasmaphysik, EURATOM Association, D-85748 Garching, Germany

1. Introduction

In the W7-AS modular stellarator (R = 2 m, $a \leq 0.18$ m, low magnetic shear), the ELM free H-mode (H*) was, until the last campaign, restricted to edge rotational transforms ι_a in the vicinity of 0.48 and 0.53 ($a \approx 0.17$ m) where the absence of low-order resonances within the edge region inside the separatrix leads to minimum magnetic pumping and thus reduced damping of the plasma poloidal rotation [1-4]. Relaxation phenomena (dithering, ELMs) were found in broader ι_a ranges [5]. After removing certain in-vessel installations which interfered with edge magnetic islands at higher ι_a, H*-scenarios with relatively strong enhancement of the stored energy are now observed also in configurations with the resonance n/m = 5/9 ($\iota_a \approx$ 0.56, $a \approx 0.14$ m) at the edge. The plasma is then bounded by relatively large magnetic islands which are intersected by the ten poloidal inboard limiters. Nevertheless, the edge region inside the separatrix is, as in the other two H-mode windows, free of low-order resonances. At high density and low to moderate heating power, the H*-mode is found to be practically unavoidable in these configurations which are of specific interest for the planned island divertor operation in W7-AS. This study gives a first overview on the observed phenomena.

2. Results, discussion and conclusions

Figure 1 plots line-averaged threshold densities $\bar{n}_e^{thr}$ for the transition to the H*-mode versus ι_a for net current-free NBI (0.4 MW) discharges, whereby the density is ramped up to the indicated values within about 0.5-0.6 s. The threshold densities are typically $\geq 10^{20}$ m^{-3} and show a slight overall-increase with ι_a. In most cases the H*-mode is preceded by relaxation phenomena such as ELMs and/or switching between L- and short (< 10 ms) H-phases. H* scenarios in ECH discharges (not shown) are restricted to the same ι_a windows but exhibit, at the same heating power, generally lower threshold densities (by up to a factor of two). H-mode effects on the confinement are shown in Fig.2 which plots τ_E normalized to τ_{ISS95} (International Stellarator Scaling [6]) versus $\bar{n}_e$ for density ramps with NBI (0.4 MW). It reflects the general tendency that the enhancement of τ_E is maximum for the island configuration at high ι_a. The example at the highest ι_a indicates a significant τ_E enhancement also for a scenario switching between short L- and H-phases. τ_E values for ECH discharges with the same heating power (not shown) match the corresponding NBI values in the L-phases, but show smaller enhancements in H*-phases which could be due to a weaker coupling to the ions.

An example for the evolution of global and edge parameters in an NBI (0.4 MW) discharge at ι_a = 0.56 is shown in Fig.3. In keeping with transport at the edge scaling with the inverse density in W7-AS [7], the electron temperatures a few centimeters inside the separatix (pedestal), and therewith the edge pressure gradients, steepen with increasing density already in the L-phase. The L-H* transition then shows well known signatures: the T_e, T_i and n_e gradients steepen further (starting at the outermost edge) leading to decreased downstream T_e values and particle fluxes onto the targets. The H_α signal (from a limiter) drops sharply and changes from “grassy“ to quiescent. Concurrently, a negative radial electric field builds up, which is consistent with the hypothesis of a transport barrier formation due to sheared $E \times B$ plasma flow [8]. T_e and n_e radial profiles (from Thomson scattering, Li-beam and ECE data;

not shown) indicate the transport barrier extends 2-3 cm inside the separatrix with pivot points slightly inside but close to the separatrix. At fixed heating power, the pedestal electron temperatures and densities at the threshold roughly follow the curve $n_e^{ped} T_e^{ped} = const.$ (Fig.4). For ECH discharges, the position on the curve depends on the ι_a window whereas NBI discharges generally show high-n_e^{ped}, low-T_e^{ped} thresholds. Assuming $T_i = T_e$, the threshold pressure gradients at the edge are of the order of 100 kPa/m at a heating power of 0.4 MW.

As already mentioned, the transition to the H*-mode is in most cases accompanied by a variety of dynamic phenomena, shown in Fig.5: **i)** Quasi periodic ELMs appear in magnetic configurations with plasma edge conditions close to the threshold of H* (see dashed lines in Fig.1 and time traces for t > 0.42 s in Fig.5). An example for these ELMs is given in Fig.6. They represent distinct transport events for particles and heat with a duration of about 200 µs, accompanied by bursts of fluctuations in density and magnetic field. For this type of discharge, the pivot point of the associated flattening of the electron temperature gradient is located about 1 cm inside the separatrix**.** Magnetic activity (f > 50 kHz) shows characteristic frequencies typically around 150 and 400 kHz which sometime behave like precursors of an ELM event (as defined by the rise of the density fluctuation level and H_α-signal) by up to 50 µs. **ii)** Switching between L and H*-states is observed for several plasma conditions (small dots in Fig.1), whereby the L-states can be considered as groups of ELM-like transport events (see time traces in Fig.4 at t < 0.4 s). In some cases this behaviour develops towards a periodic dithering with typical repetition rates up to 1 kHz and a transport effect similar to ELMs. **iii)** Small "grassy" ELM-like phenomena with a repetition rate >1 kHz, such that the spikes in H-alpha overlap in time, are observed for a much wider range of operational conditions displaying L-mode confinement (not shown).

Phases with significant relaxation phenomena could be maintained over many confinement times without significant increase of the plasma radiation. As in tokamaks, H*-scenarios are found to be generally transient. In ECH discharges, H* phases are terminated by increasing radiation followed by a reduction of edge temperatures and transitions to ELMy regimes or H*-L back transitions. In the high ι_a H-mode window with high threshold densities, the H*-phase is often terminated by a loss of density control and subsequent ECH cut-off. In NBI discharges, the H*-mode determines a (non-disruptive) radiative density limit even if the density can be kept constant after the transition. Although radiation profiles (from bolometer cameras, not shown) develop from slightly peaked in the L-phase to hollow immediately after the transition, the enhanced impurity confinement in conjunction with brader n_e-profiles then leads to quickly increasing total radiation (mainly from carbon) and subsequent thermal collapse after typically 50 – 100 ms. This limit may implicate difficulties with respect to the planned high-density island divertor studies in W7-AS. It can, however, be avoided by increasing the NBI power, which shifts the H* threshold density to higher values (Fig.7). ECH discharges at powers > 0.4 MW do not show the H* mode at accessible densities below the ECH (140 GHz) cut-off limit. The threshold $T_e^{ped} n_e^{ped}$ values (from Thomson scattering) are found to increase with heating power. This result clearly differs from the observation of a power theshold $\propto n_e B_t$ as it is generally made in tokamaks [9]. Besides the positive practical aspect concerning future high-density island divertor studies, any conclusive assessment with respect to the H-mode physics is, however, not yet possible on the basis of the present data. The power scans were, up to now, performed only for the specific configuration at $\iota_a = 0.56$. The results presented show, on the other hand, that details of the H-mode phenomenology and the occurrence of the quiescent H-mode critically vary with small changes of the rotational transform. We do not yet have an explanation, but it is conjectured that the magnetic shear profile could play a key role. The magnetic shear strongly changes with the plasma ß in W7-AS and can even invert its sign within the core. With the presently available tools, the equilibrium profiles of the rotational transform in such configurations with resonant boundaries could not be obtained with sufficient accuracy to exclude shear effects also on the observed power dependence of the H*-mode threshold. Experiments on this issue with dedicated shear modifications by externally induced plasma currents are planned.

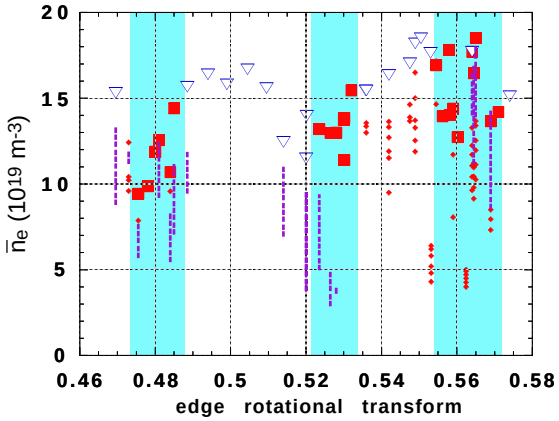

Fig.1: Threshold densities (squares) for the transition to the quiescent H-mode (H) for NBI (0.4 MW) discharges with the density ramped up at fixed ι_a. Triangles mark maximum densities without transitions. ELMy H-modes and short (1-10 ms) switching to quiescent states are indicated by dashed lines and small dots, respectively.*

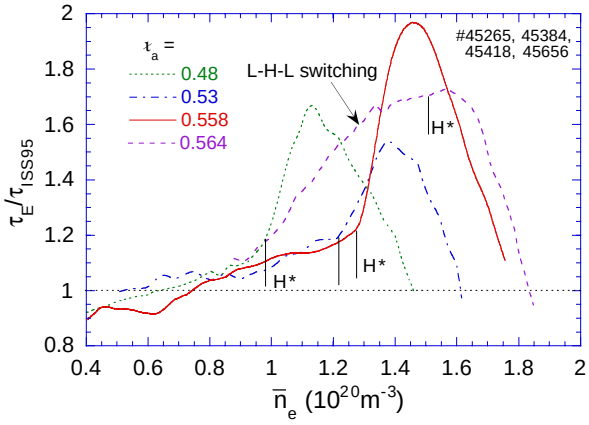

Fig..2: Energy confinement times τ_E normalized to the International Stellarator Scaling τ_{ISS95} [6] versus the line-averaged density for selected discharges of Fig.1. Transitions to the H-mode are indicated.*

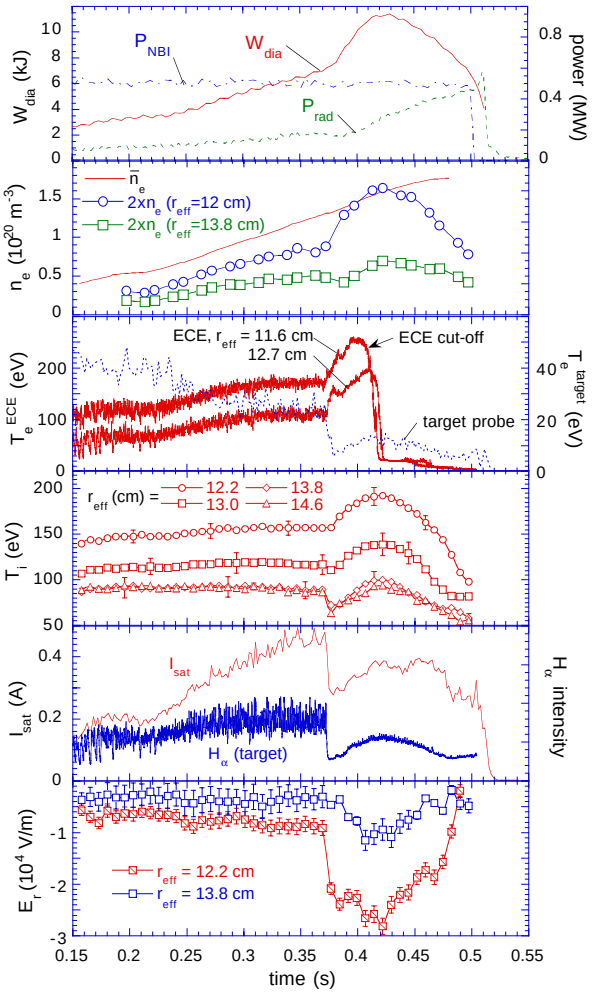

Fig.3: Evolution of global and edge parameters before and after an L-H transition in an NBI (0.4 MW) discharge at ι_a = 0.56. Densities at the edge were obtained from Li beam, ion temperatures T_i and radial electric field strengths E_r from BIV spectroscopy. The separatrix position is at an effective radius of r_{eff}=14 ± 0.5 cm.*

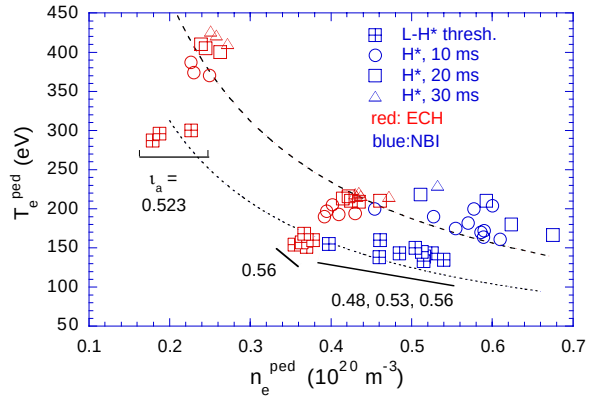

Fig.4: Electron temperatures T_e^{ped} versus densities n_e^{ped} measured 2 cm inside the separatrix (by ECE and Li-beam, respectively) immediately before, and 10, 20 and 30 ms after the transition to the H-mode. Density ramps with 0.4 MW ECH or NBI. Lines indicate $n_e^{ped}T_e^{ped}$ = const. The error of the separatrix position is estimated to be about ±5mm.*

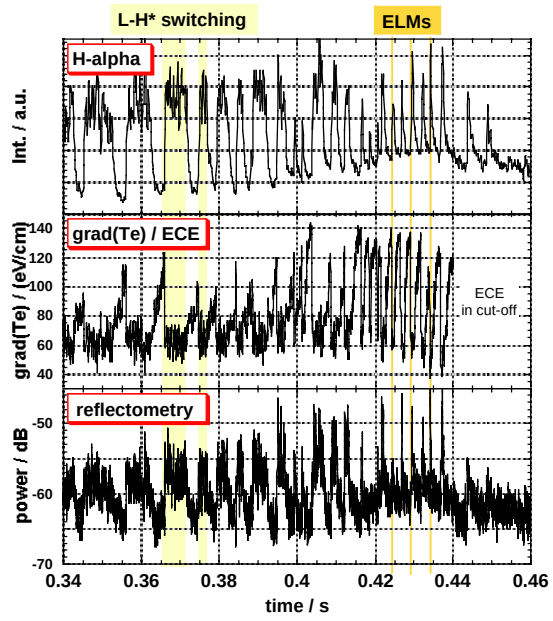

Fig.5: Plasma edge characteristics during a 100 ms time window preceeding a transition to the quiescent H-mode at ι_a=0.569: Density fluctuations at r≈a measured by reflectomery, electron temperature gradient at r=a-1cm obtained from ECE, and H-alpha signal from a limiter.

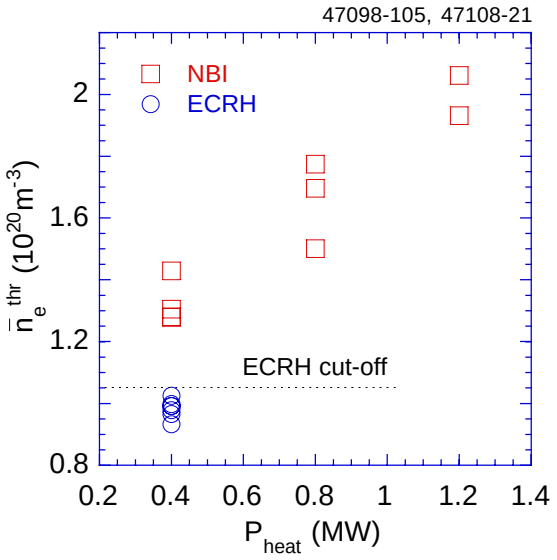

Fig.7: Threshold densities for the transition to the quiescent H-mode in dependence on the heating power for discharges in the ι_a = 0.56 configuration. For ECH (140 GHz) discharges at powers > 0.4 MW no transitions were observed within the accessible range below the cut-off density.

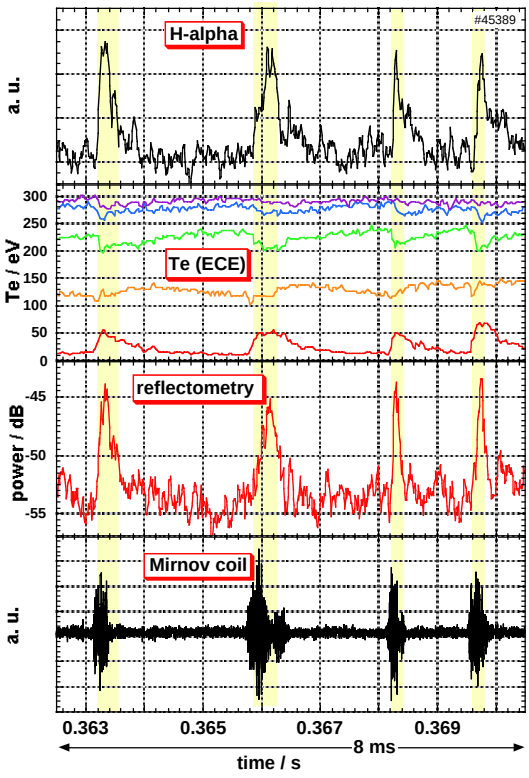

Fig.6: Plasma edge characteristics during ELMs preceeding a quiescent H-mode at ι_a=0.571: Magnetic and density fluctuations are obtained from a Mirnov coil and reflectometry respectively. The time traces of the outermost ECE channels show the edge localized character of the relaxation phenomena and their pivot point at temperatures around 100 eV, i.e. slightly inside the separatrix.

References

[1] Wagner, F. et al., Plasma. Phys. Control. Fusion **36** (1994) A61
[2[Wobig, H. and J. Kisslinger, Proc. 24th EPS Conf. (Berchtesgaden Vol. 4 (1997) 1669
[3] Hirsch, M. et al., Proc. 16th IAEA Conf. (Montreal) Vol . 2 (1996) 315
[4] Hirsch, M. et al. , Plasma Phys. Control. Fusion **40** (1998) 631
[5] Hirsch, M. et al., Proc. 25th EPS Conf. (Praha) 22C (1998) 2322
[6] Stroth, U. et al., Nuclear Fusion **36**, 8 (1996) 1063
[7] Ringler, H. et al., , Plasma Phys. Control. Fusion **32** (1990) 933
[8] Biglari, H. et al., *Phys. Fluids B* **2**,1 (1990)1
[9] Ryter, F. et al., Plasma Phys. Control. Fusion **36** (1994) A99-A104